Bottom depth carving the pelagic spatial organisation in large marine ecosystem: the case of North West Africa

Anne Mouget[1,2,*], Patrice Brehmer[3], Mohamed Ahmed Jeyid[4], Yannick Perrot[2], Ndague Diogoul[3,7], Momodou Sidibeh[5], Kamel Mamza[6], Anthony Acou[8], Abdoulaye Sarré[7]

[1] UMR BOREA Biologie des Organismes et Ecosystèmes Aquatiques, MNHN, CNRS, SU, IRD, UCN, UA, Station Marine de Dinard, CRESCO, 35800 Dinard, France

[2] Institut de recherche pour le développement, IRD, Lemar, DR ouest, Plouzané, France

[3] IRD, Univ Brest, CNRS, Ifremer, Lemar, CSRP, SRFC, Dakar, Senegal

[4] Institut Mauritanien de Recherche Océanographique et des Pêches, IMROP, BP 22, Nouadhibou, Mauritania

[5] The Fisheries Department, FD, 6 marina parade, Banjul, The Gambia

[6] Institut National de Recherche Halieutique, INRH, Casablanca, Morocco

[7] Institut Sénégalais de Recherche Agricole, ISRA, Centre de Recherche Océanographique de Dakar Thiaroye, CRODT, Pôle de recherche de Hann, Dakar, Senegal

[8] UAR Patrimoine Naturel – OFB, CNRS, MNHN – Station Marine de Dinard, CRESCO, 38 rue de Port Blanc, Dinard, France

*Corresponding author: Anne Mouget Anne.Mouget@mnhn.fr

Highlights

- Comparison of nektonic pelagic communities from shelf to offshore using fisheries acoustics data (29 586 nautical miles)
- Pelagic community structure described by echointegration profiles, scattering layers, and backscattering
- Different organization observed in inshore, transition, and offshore areas
- Key inter-annual trends identified, highlighting differences between bathymetric areas

Abstract

This study aimed to examine the spatial organization of pelagic communities within the water column along a horizontal gradient extending from the coast to the offshore area, categorized into three zones: inshore, offshore, and transition. A total of 29,000 nautical miles of acoustic transects collected during 14 annual standardized surveys were analyzed using two complementary acoustic methods: (i) extraction of sound scattering layers (SSL) and (ii) echointegration (EI) across the entire water column, both horizontally and vertically averaged. The results revealed significant differences between the three bathymetric areas based on SSL and EI descriptors, with nektonic communities in the transition area exhibiting intermediate characteristics between those in the inshore and offshore areas. The relative abundance of nektonic communities decreased from shallow coastal areas to deep offshore areas. The inshore area is different from transition and offshore area, which is confirmed by diel vertical migration (DVM) analyse through vertical profiles. All areas exhibited classic DVM type I; however, offshore and transition areas also presented unexpected DVMs of type II, *i.e.*, organisms descend deeper during the night, displaying distinct vertical profiles compared to the inshore area. This suggests that the functional and specific composition of pelagic nektonic communities differed between inshore and offshore areas, indicating that organisms adjust their responses to their environment. Over two decades, the three bathymetric areas showed a significant increase in pelagic relative biomass and variation in SSL spatial structure. Nevertheless, nektonic communities reacted differently to interannual changes depending on the bathymetric areas, such as the minimal depth of the shallowest SSL. Fluctuations in SSL descriptors were highlighted over the study period, which may be related to multi-decadal oscillations in the Atlantic Ocean.

Keywords

Sound scattering layer, bathymetry, diel vertical migration, pelagic structuration, interannual trends.

1. Introduction

Bathymetry is recognized as a structuring environmental factors for fish communities (Louisy, 2015), phytoplankton communities (Huan *et al.*, 2022), and is utilized in various models (Hedger *et al.*, 2004; Kaschner *et al.*, 2006; Lenoir, Beaugrand and Lecuyer, 2011). Marine organisms are constrained by bathymetry, but they also follow patterns that exhibit temporal fluctuations according to diel vertical migration (DVM), interannual variations (Lenoir, Beaugrand and Lecuyer, 2011), and long-term trends (Beaugrand, Ibañez and Reid, 2000; Brunel and Boucher, 2007).

The Canary Current Large Marine Ecosystem (CCLME) is situated along the West African coasts from 10°N to 40°N (Spall, 1990). Economically important for countries (Görlitz and Interwies, 2013; Diankha *et al.*, 2017; Sarré *et al.*, 2018), the CCLME's functioning is quite complex, depending on depth, latitude, coast specificity, and upwelling events (Diogoul *et al.*, 2021). Previous studies on the CCLME (Barton *et al.*, 1998; Arístegui *et al.*, 2009; Auger *et al.*, 2016) do not highlight the effect of upwelling on other environmental aspects on pelagic organism spatial structuration. Bottom depth is an environmental variable that well explains marine community structure (Majewski *et al.*, 2017). The way depth controls the spatio-temporal organization of pelagic communities over the continental shelf remains poorly understood.

The most common method to describe the spatial organization of nektonic and zooplanktonic communities in the marine environment is based on non-intrusive acoustic surveys (Simmonds and MacLennan, 2005; Brehmer *et al.*, 2019). In this study, we used 14 acoustic sea surveys carried out over 21 years. Such a long-term dataset allowed us to study inter-annual variability and gain potential first insights into climate change effects. To analyze the organization of aggregating pelagic organism communities, we used Sound Scattering Layers (SSL) descriptors (Mouget *et al.*, 2022). SSLs are aggregations of micronekton, macrozooplankton, and many other pelagic organisms, which play a key trophic role in pelagic ecosystems (Remond, 2015; Béhagle *et al.*, 2017; Blanluet *et al.*, 2019). They are, therefore, structures that can be used as sentinels in marine ecosystems (Remond, 2015) as they are sensitive to spatial and long-term environmental changes (Hays, Richardson and Robinson, 2005). SSLs are also used to understand patterns of organization, such as diel vertical migrations (DVM) (Benoit-Bird and Au, 2004) and monitor the ecological state of ecosystems (Diogoul *et al.*, 2021). Besides SSLs, echointegration-based descriptors (Perrot *et al.*, 2018) collected from the water column are complementary thanks to their comprehensive scan of the water column, enabling the inclusion of organisms distributed outside the SSLs.

With our large spatial coverage and fine resolution dataset, pelagic organism distribution patterns are compared between bathymetric areas and their inter-annual variability is analyzed. As fisheries acoustics are the most reliable (requiring low standardization) and available time series, particularly in poor data ecosystems, this study aims to evaluate, based on fisheries acoustics time series and without biological sampling, how bottom depth influences pelagic organization, considering independently three distinct areas commonly discriminated in fisheries sciences: the inshore, transition, and offshore areas.

2. Material and methods

2.1. Material

Acoustic data were collected using a 38 kHz transceiver type ES38-B on-board R/V Dr. Fridtjof Nansen with the following settings: at a depth of 5.5 m, an absorption coefficient of 8.7 dB km-1, a pulse length of 1.024 ms, and a maximum transmission power of 2000 W (Krakstad et al., 2006; Sarré et al., 2018). The echosounder was annually calibrated following the classic calibration procedure (Foote *et al.*, 1987) using a standard copper sphere for 38 kHz. Data were recorded over the Canary Current Large Marine Ecosystem (CCLME). The CCLME is one of the 64 large marine ecosystems (LMEs) defined worldwide to propose ecologically rational units of ocean space (Sherman, 1994). While the CCLME presents a global homogeneity, two areas, the North and South CCLME, can be discriminated against with either permanent or seasonal upwelling, respectively (Barton, Field and Roy, 2013; Benazzouz *et al.*, 2014). CCLME is highly productive and allows the study of pelagic spatial structuration mainly due to small pelagic fish and zooplankton. However, this area exhibits a wide range of environmental conditions, influenced by currents (Faye *et al.*, 2015), as well as local factors such as river plumes and coastal influences, impacting crucial parameters like sea temperature and macronutrient concentrations. Seasonal upwelling occurs during the summer in the South CCLME (Benazzouz *et al.*, 2014) and a permanent upwelling occurs in the North part. To work on a homogeneous ecosystem, we reduce the dataset to the South part of CCLME, without upwelling impact.

Hereafter we referred to the South part of CCLME as "SCCLME." The study area extended from the southern border of Senegal (12.15°N) to Cape Blanc (20.77°N) and from longitude 16°W to 18°W (Figure 1).

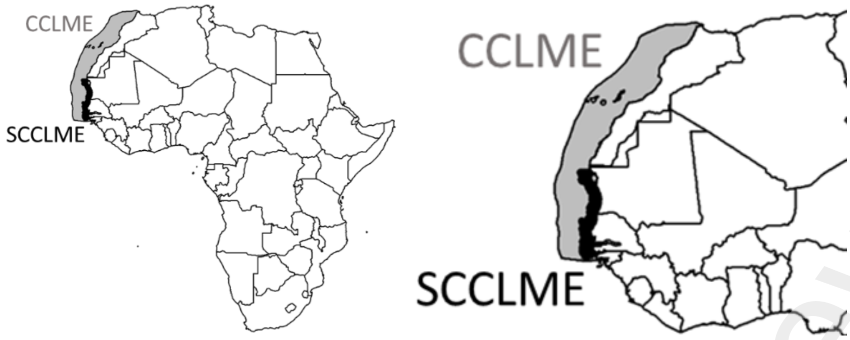

Figure 1. Map of the Canary current large marine ecosystem (CCLME in grey) in the African Topical Atlantic Ocean, including the study area, named here the South part of the CCLME (SCCLME in black: Mauritania, Senegal and The Gambia).

To focus on the influence of bathymetry on the acoustic signal without interfered from upwelling regimes, our study area was limited to the SCCLME outside the permanent upwelling (Gómez-Letona *et al.*, 2017). All surveys included in this study were conducted during the wet season (November and December) between 1995 and 2015, totaling 29,586 nautical miles (nmi) analyzed. The survey designs remained consistent over the years (Figure 2), and surveys were conducted 24/24, covering day, night, and transitional periods. Transitional periods were defined using sun altitude, calculated based on date, time, and geographic position. Diel transition periods corresponding to sunset and sunrise, with a sun altitude between -18° and +18° (Lehodey *et al.*, 2015; Perrot *et al.*, 2018), were excluded from analyses to avoid density change bias due to diel vertical migrations (DVM).

The data were categorized into three bathymetric areas: inshore, transition, and offshore. The bottom depth was defined using acoustic data. The bottom depth has been estimated using the software Matecho using a backstep minimum level of -50 dB, and then manually post processed to correct bottom line errors. Inshore corresponds to the shelf, close to the coasts, with a depth under 150 m. The transition includes bottom depths between 150 and 500 m, encompassing a deeper continental shelf and the slope. Offshore areas were defined as having bottom depths ranging from 500 to 1500 m. This zonation is commonly used in studies, aligning with physical and biological functioning (e.g., Gibson, Atkinson and Gordon, 2005; Castillo, Ramil and Ramos, 2017). Fisheries acoustics data were clustered into elementary sampling units (ESUs) of 0.1 nautical miles (nmi) (Table 1).

Table 1. Summary of the dataset collected during sea surveys on-board the R/V Dr. Fridtjof Nansen over the South part of the Canary Current Large Marine Ecosystem between 1995 and 2015. The number of Elementary Sampling Units (ESU) of 0.1

nautical miles (n= 295 860) are detailed for inshore (bottom depth < 150 m), transition (bottom depth from 150 to 200 m), and offshore (bottom depth > 500 m) areas.

Year	Number of ESUs (0.1 nmi)			
	Inshore	Transition	Offshore	Total
1995	4 514	9	19 636	24 159
1996	3 107	1 303	17 663	22 073
1997	2 044	1 186	15 338	18 568
1998	2 479	1 695	16 093	20 267
1999	2 858	2 286	12 597	17 741
2000	3 590	2 379	16 385	22 354
2001	2 323	4 557	15 451	22 331
2002	6 401	475	17 757	24 633
2003	2 620	3 275	16 251	22 146
2004	2 745	2 699	15 253	20 697
2005	2 292	2 651	18 546	23 489
2006	3 196	2 431	14 971	20 598
2011	4 077	2 501	8 383	14 961
2015	5 531	943	15 666	22 140
Total	47 480	28 390	219 990	295 860

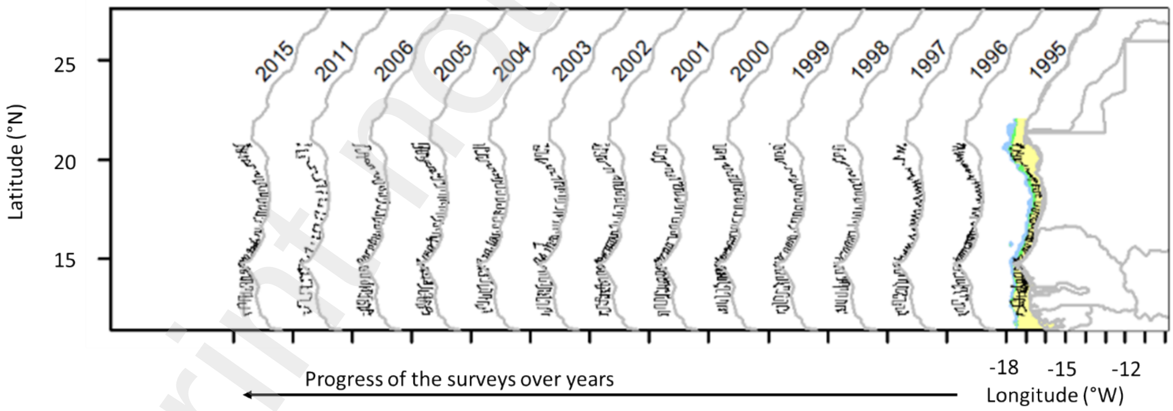

Figure 2. Map of the acoustic survey sampling per year and bathymetry along the African coast (Mauritania, Senegal, and Gambia) in the Canary Current Large Marine Ecosystem. The acoustic sampling design is drawn in black along the coastline in grey The continental shelf bathymetry is presented using a colour scale: In yellow, inshore (bottom depth < 150 m); in green, transition (bottom depth in 150-500 m); and in blue, offshore (bottom depth > 500 m).

2.2. Methods

The dataset was analyzed using two methods: (i) horizontally or vertically averaged echointegrated echograms; and (ii) extracted Sound Scattering Layers (SSLs). Echointegration was conducted using a threshold of -100 dB to include everything in the water column. SSLs were extracted using Matecho (Perrot *et al.*, 2018) from echointegrated echograms using a segmentation algorithm at an echo level threshold of -70 dB re 1 m^{-1}, denoted as dB hereafter. The -70 dB threshold was chosen to encompass both the micronektonic layers (Béhagle *et al.*, 2016) and the contribution of pelagic fish. SSL descriptors were computed per ESU of 0.1 nmi to characterize SSLs in the water column up to a depth of 500 m. Matecho computed six descriptors per ESU for each SSL.

Descriptors were selected to facilitate efficient analysis for comparing ecosystems at different depths and were based on the shallowest SSL and all SSLs (Mouget *et al.*, 2022). The shallowest SSL is the most independent SSL of the bottom depth, i.e., it is the farthest from the bottom. Moreover, Mouget *et al.*, (2022) highlighted that there were few ESUs with more than one SSL over the shelf. In addition to the shallowest SSL analysis, descriptors based on the entire water column or all SSLs were also used, added to the SSL descriptors (Table 2): (i) the mean volume backscattering strength (S_v in dB) from echointegrated echograms ($S_{v,\ EI}$) allowing an analysis of the whole water column; (ii) the S_v of shallowest SSL ($S_{v,\ 1}$) to analyse the acoustic importance of the shallowest SSL; (iii) the mean S_v of all SSLs ($S_{v,\ all}$) to have a complete view on all SSL along the water column; (iv) the minimal depth of the shallowest SSL ($đ_1$); (v) the width of shallowest SSL ($\dot{W}_1$) to identify the behaviour of shallowest SSL; (vi) the number of SSLs (Ŋ) on the organisation of the water column. $S_{v,\ EI}$, $S_{v,\ 1}$, $S_{v,\ all}$, $đ_1$, $\dot{W}_1$, and Ŋ are referred to as descriptors from here. S_v (dB) serves as a proxy for pelagic biomass (Holland *et al.*, 2021; Ariza *et al.*, 2022), hereafter referred to as pelagic biomass.

Table 2. Descriptors used in this study, their symbols, units, formulas, and or reference(s). S_v is the volume backscattering coefficient in dB and s_v is the volume backscattering coefficient in m^{-1} *(MacLennan, Fernandes and Dalen, 2002)*. N/A means not applicable. "i" is the sound scattering layers (SSL) number, starting at 1 for uppers SSL in surface, and "j" is the Elementary Sampling Unit (ESU) number.

Denomination of descriptors	Symbol	Unit	Formulae	Reference(s)
Bottom depth at ESU j	D_j	Meter (m)	N/A	-
Number of echointegrated cells at ESU j	N_j	-	N/A	-

Number of SSL at ESU j	$Ŋ_{j}$	-	N/A	Urmy *et al.* (2012); Weill *et al.* (1993); Woillez *et al.* (2007)
Mean S_v from echointegrated echograms at ESU j	$S_{v, EI, j}$	Decibel (dB)	10	MacLennan *et al.* (2002)
S_v of shallowest SSL at ESU j	$S_{v, 1, j}$	Decibel (dB)	10	Mouget *et al.* (2022 adapted from MacLennan *et al.* (2002)
Mean S_v of all SSLs at ESU j	$S_{v, all, j}$	Decibel (dB)	10	Mouget *et al.* (2022) adapted from MacLennan *et al.* (2002)
Minimal depth shallowest SSL at ESU j	$đ_{1, j}$	Meter (m)	N/A	Mouget *et al.* (2022)
Width of shallowest SSL at ESU j	$\dot{W}_{1, j}$	Meter (m)	N/A	Mouget *et al.* (2022)

The dataset's spatial auto-correlation along transects was considered negligible (Domokos, 2009; Sabarros *et al.*, 2009; Béhagle *et al.*, 2014). Statistical analyses were conducted using R version 4.3.2 (R Core Team, 2021).

Kernel density was computed for each SSL descriptor ($S_{v, 1}$, $S_{v, all}$, $đ_1$, $\dot{W}_1$) and echointegration descriptor ($S_{v, EI}$). Kernel density estimation (Sheather and Jones, 1991; Zhang *et al.*, 2018) was employed to construct probability density functions. To compare the densities from descriptors and variations of Sv, EI with respect to depth, two tests were used. The Wilcoxon test compared means (Fay and Proschan, 2010), while the Spearman correlation test estimated the degree of correlation between two curves (Croux and Dehon, 2010). For discrete descriptors, *i.e.*, the number of SSLs (Ŋ), the Chi-square test was employed (McHugh, 2013). All statistical tests were conducted with a significance threshold of 0.05 for the *p*-values. The analysis of different acoustic descriptors allowed the examination of the relative importance of acoustic density within and outside of SSLs, as well as the difference between the shallowest and all SSLs, highlighting variations in water column organizations.

Vertical profiles were computed using the complete dataset of S_v from echointegration, consisting of data for each cell of one ESU length (0.1 nmi) by 1-meter depth. For each year, a vertical profile was computed as the mean of all data at each depth with an accuracy of 1 m depth. When there were fewer than 50 ESUs, no mean was computed to avoid unreliable outliers. Vertical profiles for each year were then averaged to produce a single curve for each depth category (inshore, transition, offshore). To compare patterns of vertical profiles, the datasets were truncated to the length of the smallest profile, i.e., the length of the shelf profile, up to 150 m. Correlations between curves were calculated using the Spearman coefficient (Kendall, 1938). The mean difference between the two curves was determined by averaging the differences at each point.

To assess the relative importance of acoustic classes in inshore, transition, and offshore areas, another analysis was performed. For each survey, each cell of 1 ESU length by 1-meter width was assigned to one of four $S_{v,\,EI}$ classes based on S_v values between arbitrary limits of ten dB intervals: [-50; -60[, [-60; -70[, [-70; -80[, [-80; -90] dB as defined by Mouget *et al.* (2022). Cells with values outside were excluded. The relative importance of each class was then calculated per bathymetric area by dividing the number of cells in an $S_{v,\,EI}$ class by the number of classified cells in the corresponding ESU.

To perform DVM analysis, densities of $S_{v,\,EI}$, $S_{v,\,1}$, and $S_{v,\,all}$ were computed using the Kernel density method (Sheather and Jones, 1991; Silverman, 1986) for each bathymetric area separately during the day and night periods. The day density was then subtracted from the night density to obtain a single differential curve for each inshore, transition, and offshore area. The curves were analyzed using the same method as vertical profiles.

To analyze changes over decades and inter-annual changes, linear regressions and polynomial regressions of orders 2 and 3 were calculated using years as the single explicative variable (Mouget *et al.*, 2022). We selected the best regression model ($p < 0.05$) based on the Akaike Information Criterion (AIC) by comparing models trained on a portion of the data (50%) and validated on the remaining data (50%).

3. Results

3.1. Comparison of SSL and echointegration descriptors by bathymetric areas

3.1.1. Comparison of descriptors

The density curves (Figure 3a, b, c) exhibited distinct patterns for all acoustic ($S_{v,\,EI}$, $S_{v,\,1}$, $S_{v,\,all}$) across the three bathymetric areas. Inshore had maxima for higher values of Sv than transition and offshore. The inshore's maxima were at -64.4, -63.5, and -63.7 dB for $S_{v,\,EI}$, $S_{v,\,1}$, and $S_{v,\,all}$, respectively, while maxima for the offshore area shifted towards lower values with -74.0, -64.5, and -66.5 dB, respectively. Peaks of the transition area were close to offshore ones, with peaks at -73.9, -64.7, and -67.3 dB for $S_{v,\,EI}$, $S_{v,\,1}$, and $S_{v,\,all}$,, respectively. Although the correlation between the curves was not significant, all curves were single-modal. The shift between the inshore and other curves (transition and offshore) was more pronounced for $S_{v,\ EI}$ with a difference of almost 10 dB (-64.4 dB inshore vs -74.0 and -73.9 dB in transition and offshore, respectively).

For descriptors based on the shallowest SSL (đ$_1$ and Ẇ$_1$), transition and offshore presented similar curves. The inshore curve is similar but with a higher kernel density for inshore at the maxima. The curves were not significantly correlated. The number of SSLs (Ŋ) revealed two different spatial organizations. The first one occurred in transition and offshore areas and was characterized by an increase in the percentage of ESUs from zero to two SSLs (an increase from 2.8% (Ŋ = 0) to 35.4% (Ŋ = 2) and from 1.5% (Ŋ = 0) to 35.9% (Ŋ = 2) for transition and offshore, respectively). The second behavior was observed only in the inshore, with an increase in the percentage of ESUs only up to one SSL. Inshore had 84.7% of ESUs with only one SSL, whereas ESUs from transition and offshore were more distributed between all numbers of SSLs (with a maximal percentage of 38.5% and 35.9% for transition and offshore, respectively).

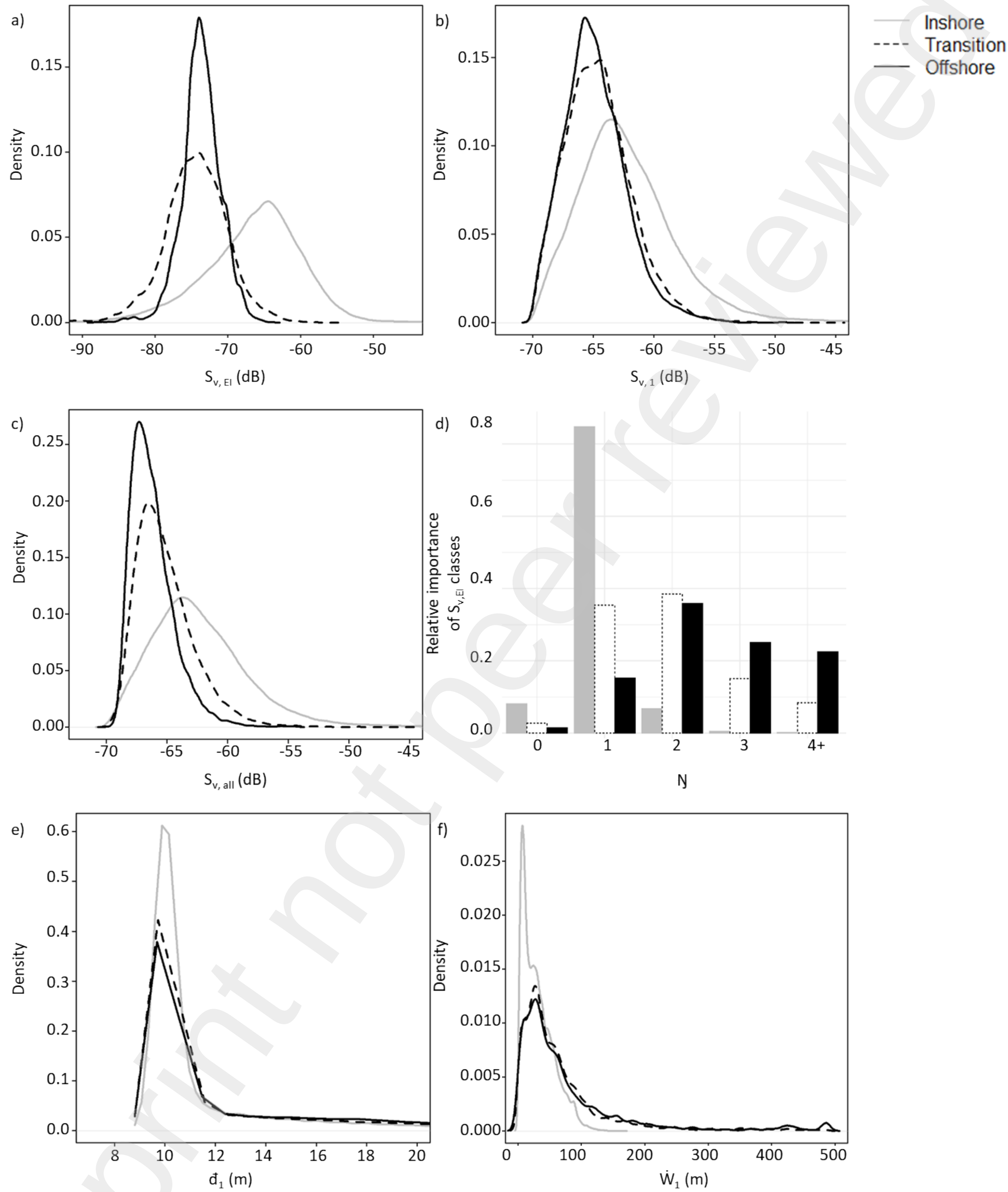

Figure 3. Comparison of differences between Kernel density curves for the three bathymetric areas, for all surveys analysed (1995-2015). a) Mean volume backscattering coefficient S_v (in dB) from echointegrated echograms ($S_{v, EI}$); b) S_v of shallowest sound scattering layer ($S_{v, 1}$); c) S_v of all sound scattering layers ($S_{v, all}$). The bathymetric areas are represented as follows. In full grey, the inshore (bottom depth < 150 m). In dotted black, the transition (bottom depth in 150-500 m). In full black, the offshore (bottom depth > 500 m). d) Relative importance of elementary sampling units (ESU) with 0, 1, 2, 3 or more (4+)

number of sound scattering layers (Ŋ) by bathymetric area. e) Minimal depth of shallowest sound scattering layer ($đ_1$). f) Width of shallowest sound scattering layer ($\dot{W}_1$).

3.1.2. Vertical profiles of $S_{v,\,EI}$

The three vertical profiles of $S_{v,\,EI}$ exhibited similar patterns across all three bathymetric areas (Figure 4). Correlation tests between the three profiles were significant, with a correlation coefficient greater than 0.95. However, inshore vertical profiles displayed higher $S_{v,\,EI}$ values from the surface to 100 m depth. The mean difference between inshore and transition profiles was 2.4 dB for depths up to 150 m and 2.6 dB for depths up to 150m between inshore and offshore profiles. The mean difference between transition and offshore was 0.18 dB for depths up to 100 m and 0.93 dB for depth up to 500 m. Additionally, we observed that the S_v values were higher in the offshore area than in transition areas up to a depth of 200 m depth, after which the transition area exhibited higher values of S_v.

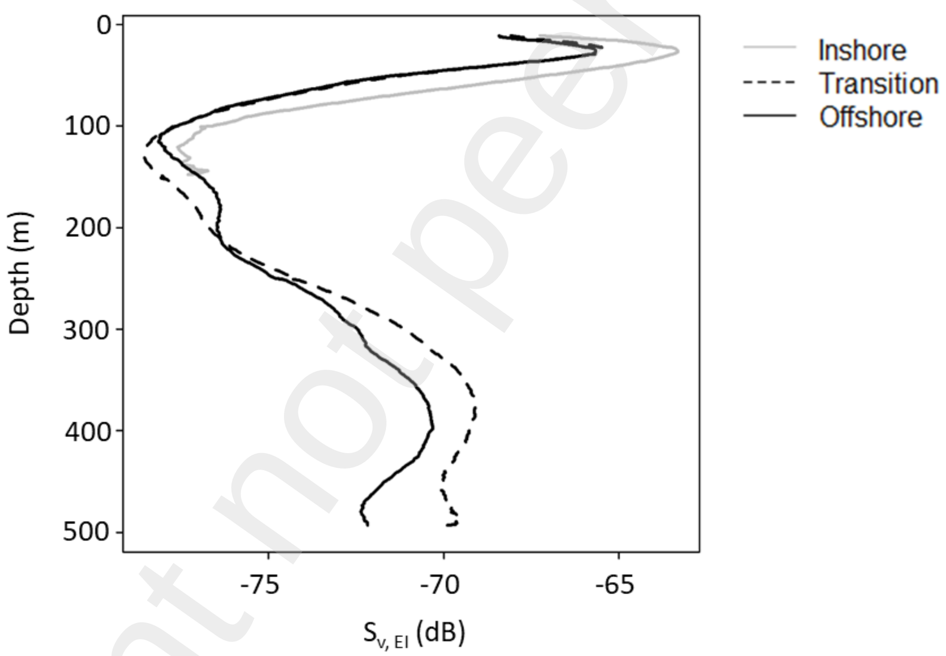

Figure 4. a) Vertical profiles of mean S_v from echointegrated echograms ($S_{v,\,EI}$) of all survey years (0-500 m). In full grey, the inshore (bottom depth < 150 m). In dotted black the transition (bottom depth [150-500 m]). In full black, the offshore (bottom depth > 500 m).

3.2. Comparison of $S_{v,\,EI}$ classes per bathymetric areas

The comparison of the relative importance of $S_{v,\,EI}$ classes across different depth categories revealed interesting patterns across the three bathymetric areas (Figure 5). Inshore areas had a higher proportion of the class [-60; -50[(11.6%) compared to transition (3.8%) and offshore areas (2.3%). Conversely, the $S_{v,\,EI}$ classes [-80; -70[and [-90; -80[dB were more abundant in transition (47.9% and

20.0%, respectively) and offshore areas (52.5% and 15.6%, respectively) compared to inshore (35.5% and 10.8%, respectively). The class [-70; -60[dB was the most abundant in all areas, with inshore (40%) having the highest proportion and transition and offshore (46 and 51%, respectively) having the highest proportion for [-80; -70[dB. The similarities between transition and offshore areas were evident, especially for the lower proportion of the class [-70; -60[dB (28.3 and 29.6%, respectively) compared to inshore (42.2%). These proportions were significantly independent of the three bathymetric areas, even though transition and offshore showed similar distributions.

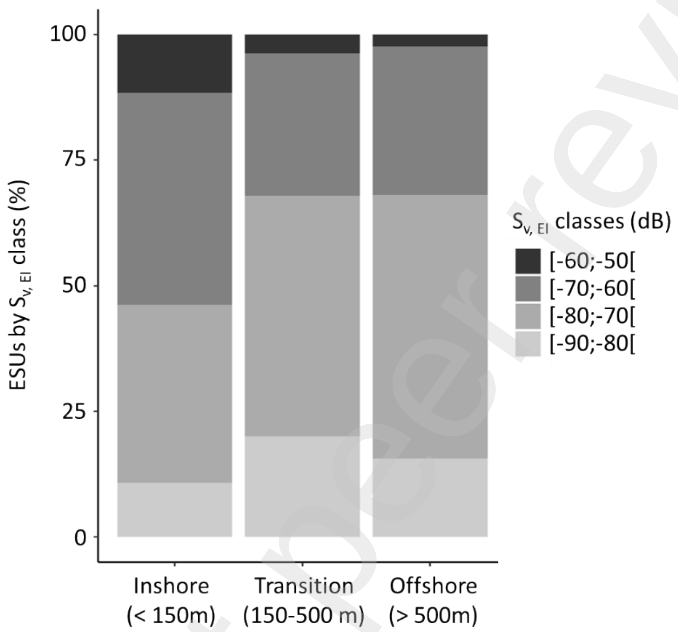

Figure 5. Comparison of percentage of Elementary Sampling Unit (ESU of 0.1nmi, n = 295 860) in each category of mean volume backscattering strength (S_v in dB) from echointegrated echograms ($S_{v,EI}$) for all surveys conducted from 1995 to 2015, across the inshore (depth < 150 m), transition (depth in 150-500m) and offshore (depth > 500 m) areas. The $S_{v,EI}$ classes are represented as follows: light grey: $S_{v,EI}$ class in the range [-90; -80[dB; in grey, [-80; -70[dB; in dark grey, [-70; -60[dB; and in black, [-60; -50[dB.

3.3. Comparison of DVM per bathymetric areas

3.3.1. Diel Vertical Migration through comparison of descriptors

Mean S_v ($S_{v,EI}$) exhibited different patterns according to the bathymetric area considered. The patterns were similar in inshore and transition areas (significant Spearman coefficient of 0.91) (Figure 6a). They both had a peak with negative values of density difference (-0.032 at -72 dB and -0.022 at -78 dB, for inshore and transition areas, respectively) followed by a positive peak. The offshore curve had a different shape, with two negative and two positive peaks.

The DVMs of the shallowest SSL, $S_{v,\,1}$, varied according to similar patterns, whatever the bathymetric area (Figure 6b). However, the lowest DVM values were observed for inshore areas than for both offshore and transition areas.

The DVMs of all S_v SSLs ($S_{v,\,all}$, Figure 6c) showed similar patterns to the shallowest SSLs ($S_{v,\,1}$, Figure 6b). Indeed, the DVMs shifted from negative to positive values at a threshold of 0.64 and peaked at -0.6 dB for $S_{v,\,all}$ = 68 dB, and peaked at +0.3 and +0.2 for offshore and transitional areas, respectively. Noteworthy, these DVMs were less marked than for shallowest SSLs.

The difference in the relative importance of $S_{v,\,El}$ classes (Ŋ) between day and night was limited to 8% in transition and offshore areas whatever the number of SSLs, whereas they were much higher inshore, where they reached up to 62% (Figure 6d). This highlighted high changes in the number of SSLs between day and night in the inshore area.

All density differences were positive or close to zero for $đ_1$, whatever the bathymetric area and the depth of the shallowest SSL (Fig 6e). This indicates that minimum depths were shallower during nighttime than during daytime. For all bathymetric areas, the density difference decreased with the depth of the shallowest SSL. Interestingly, the highest differences were observed in the transition area, followed by offshore and inshore areas suggesting that vertical movements have a higher amplitude in the transition area than both in offshore and inshore areas.

Differences in SSL widths ($\dot{W}_1$, Figure 6f) have similar patterns in transition and offshore, positive from 43 m width. This means that during the daytime, there were more SSLs with a width under 43 m than during nighttime. Therefore, SSL was thinner during the daytime. Inshore, the difference is positive from 10 m width. Therefore, the width of SSLs did not change between day and night for large SSLs (with a width over 10 m).

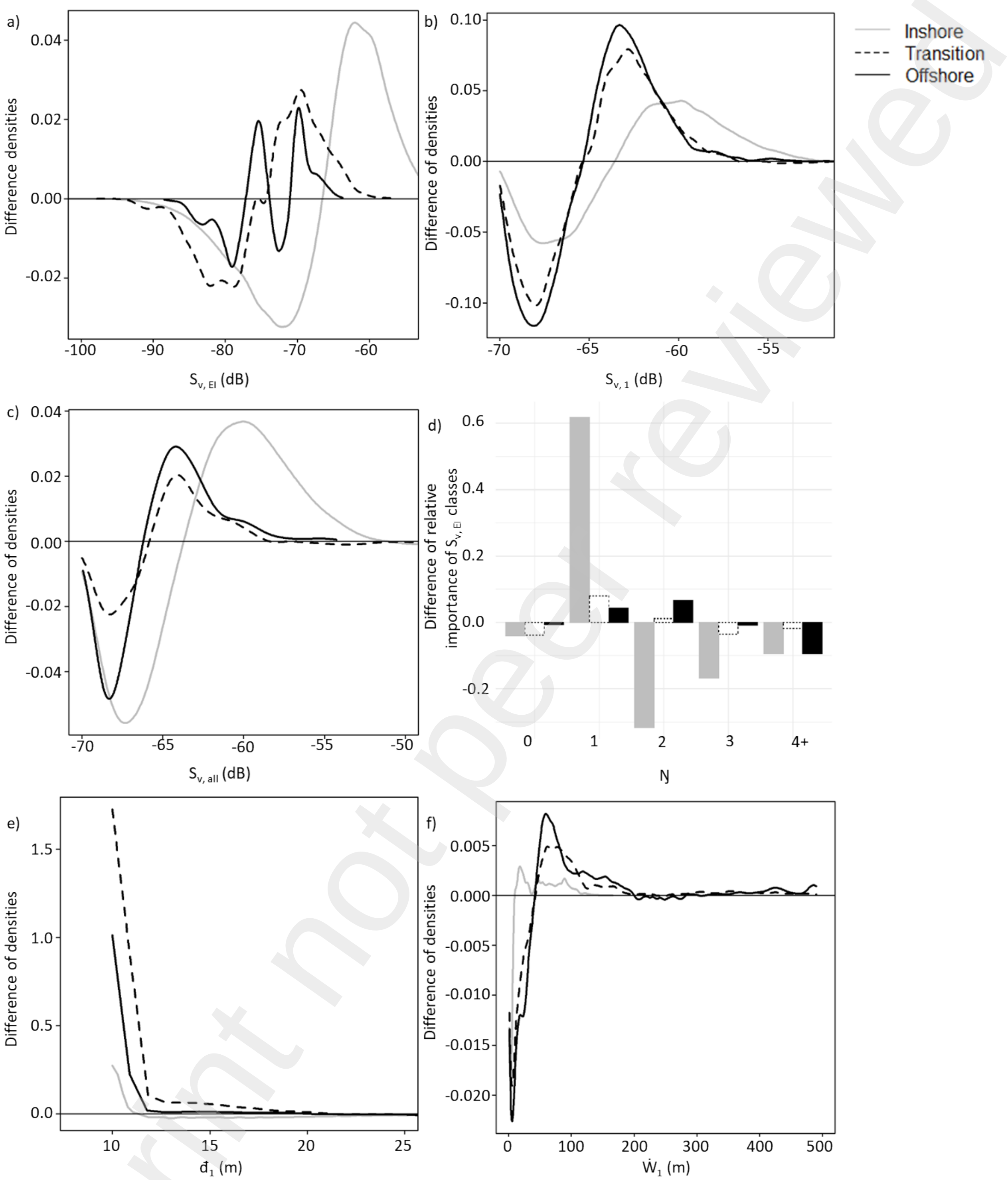

Figure 6. Comparison of difference between density curve of night and day (all surveys 1995-2015) for the three bathymetric areas. In full grey, the inshore (depth < 150 m); in dotted black, the transition (depth in 150-500 m); in plain black, the offshore area (depth > 500 m). a) Mean S_v from echointegrated echograms ($S_{v,\,EI}$); b) S_v of shallowest sound scattering layer ($S_{v,\,1}$); c) mean S_v of all sound scattering layers ($S_{v,\,all}$); (d) difference between relative number of SSLs (Ŋ) between nighttime and daytime; e) minimal depth of shallowest sound scattering layer ($đ_1$); f) width of shallowest sound scattering layer ($\dot{W}_1$);

3.3.2. Diel Vertical Migration through vertical profiles of $S_{v, EI}$

The analysis of vertical profiles of $S_{v, EI}$ of DVM (Figure 7ab) showed similar patterns between transition and offshore areas, with a strong significant correlation coefficient of 0.90 observed between the two profiles. In contrast, the vertical profile from the inshore area showed an inverse correlation to both transition and offshore areas. Notably, significant negative correlation coefficients of -0.53 and -0.77 were observed for transition and offshore areas, respectively.

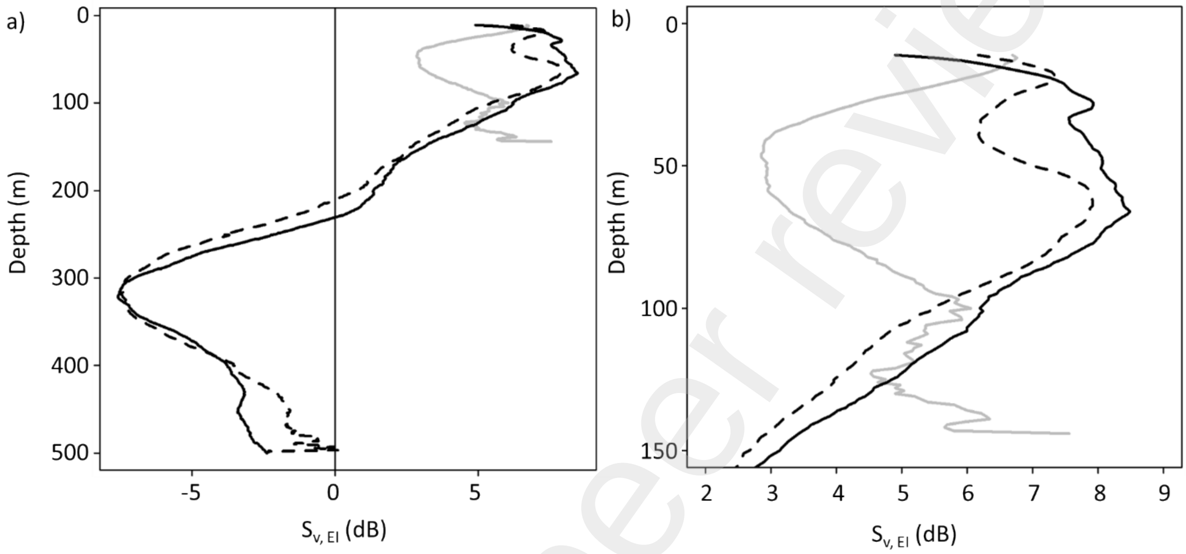

Figure 7. Differential vertical profiles of mean volume backscattering strength (S_v in dB) from echointegrated echogram ($S_{v, EI}$) for all surveys (1995-2015). The profiles were obtained by subtracting night-time from daytime echograms for the following depth ranges: a) all depths (0-500 m). b) Zoom on 0-150 m depth. The bathymetric areas are indicated as follows: full grey, the inshore (bottom depth < 150 m); in dotted black, transition (bottom depth in 150-500 m); in plain black, offshore (bottom depth > 500 m).

All statistical tests, including DVM comparison, comparing eight descriptors in pairs between inshore, transition, and offshore were computed, revealing 27 significant differences out of 45 tests conducted (Table 3). Thirteen tests analyzing the difference between day and night were significant out of 21 tests conducted. These tests also highlight the high correlation between transition and offshore for the shallowest SSL (with Spearman coefficient ranging from 0.78 to 0.90). When the entire water column was included ($S_{v, EI}$ and $S_{v, all}$), the correlation between transition and offshore was less important (0.56 and 0.48, respectively). DVM was significantly different inshore, with no correlation with other bathymetric areas.

Table 3. Statistical analysis comparing descriptors (by pair) between inshore, transition, and offshore areas for a full diel cycle (global analyses) and for the difference between daytime and nighttime (diel vertical migration analyses). Note:

Wilcoxon and Spearman tests were conducted for continuous data, while the Chi-square test was used for discrete data (N and $S_{v, EI}$ classes). “ns” indicates non-significant results. “SSL” refers to sound scattering layer. Significant p-values < 0.05.

Descriptor	Symbol	Compared bathymetric area	Wilcoxon test or chi-square *p*-value	Spearman coefficient
Global analyses (including day and night)				
Mean S_v from echointegrated echograms	$S_{v, EI}$	Inshore - transition	< 0.05	0.97
		Transition - offshore	< 0.05	0.97
		Inshore - offshore	< 0.05	0.96
S_v of shallowest SSL	$S_{v, 1}$	Inshore - transition	< 0.05	0.96
		Transition - offshore	< 0.05	0.98
		Inshore - offshore	< 0.05	0.93
Mean S_v of all SSLs	$S_{v, all}$	Inshore - transition	< 0.05	0.97
		Transition - offshore	< 0.05	0.92
		Inshore - offshore	< 0.05	0.86
Number of SSLs	Ŋ	Inshore - transition	ns	-
		Transition - offshore	ns	-
		Inshore - offshore	ns	-
Minimal depth shallowest SSL	đ$_1$	Inshore - transition	ns	0.25
		Transition - offshore	ns	0.78
		Inshore - offshore	ns	ns
Width of shallowest SSL	Ẇ$_1$	Inshore - transition	< 0.05	0.94
		Transition - offshore	< 0.05	0.83
		Inshore - offshore	< 0.05	0.82
Vertical profiles of $S_{v, EI}$	n/a	Inshore - transition	< 0.05	0.99
		Transition - offshore	ns	0.95
		Inshore - offshore	< 0.05	0.96
$S_{v, EI}$ classes	n/a	Inshore - transition	ns	-
		Transition - offshore	ns	-
		Inshore - offshore	ns	-
Diel Vertical Migration Analyses (difference between daytime and nighttime)				
Mean S_v from echointegrated echograms $S_{v, EI}$	$S_{v, EI}$	Inshore - transition	ns	0.91
		Transition - offshore	ns	0.56
		Inshore - offshore	ns	0.12
S_v of shallowest SSL	$S_{v, 1}$	Inshore - transition	< 0.05	0.47
		Transition - offshore	< 0.05	0.78
		Inshore - offshore	< 0.05	0.41
Mean S_v of all SSLs	$S_{v, all}$	Inshore - transition	< 0.05	0.56
		Transition - offshore	< 0.05	0.48
		Inshore - offshore	< 0.05	0.33
Number of SSLs	Ŋ	Inshore - transition	ns	-
		Transition - offshore	ns	-
		Inshore - offshore	ns	-
Minimal depth shallowest SSL	đ$_1$	Inshore - transition	< 0.05	-0.13
		Transition - offshore	< 0.05	0.83
		Inshore - offshore	ns	ns
Width of shallowest SSL	Ẇ$_1$	Inshore - transition	< 0.05	0.31
		Transition - offshore	ns	0.84
		Inshore - offshore	< 0.05	0.24
Vertical profiles of $S_{v, EI}$	n/a	Inshore - transition	< 0.05	-0.53
		Transition - offshore	< 0.05	0.90
		Inshore - offshore	< 0.05	-0.77

3.4. Inter-annual trend per bathymetric areas

All indicators showed significant shifts between 1995 and 2015, following either linear trends or polynomial trends. Notably, the mean pelagic biomass ($S_{v,1}$, $S_{v,all}$, and $S_{v,EI}$) increased significantly over time in all areas. In the inshore area (Figure 8a) $S_{v,EI}$ increased from -67.5 dB in 1995 to -66 dB in 2000. In the offshore and transition areas (Figure 8b, c), the pelagic biomass showed a significant linear increase throughout the entire period, reaching maximum values of -72 and -74 dB in 2005 in the transition area and offshore, respectively.

The shallowest SSL, as measured by $S_{v,1}$, displayed distinct patterns depending on the area. In the inshore area, it followed a Gaussian-like curve with a peak in 2005 (Figure 8d). No significant trend was observed in the transition areas (Figure 8e). Offshore, $S_{v,1}$ exhibited a hyperbolic trend with low values in 2005 and peak values in 1995 and 2005 (Figure 8e).

The mean patterns of all SSL ($S_{v,all}$) mirrored the patterns of $S_{v,1}$ for the inshore (Figure 8g) and offshore (Figure 8i) areas. However, in the transition area (Figure 8h), the $S_{v,all}$ pattern resembled that of the inshore area, with a S_v peak observed in 2004-2005.

The number of SSLs (Ŋ) increased in all areas (Figure 8j, k, l). Inshore, Ŋ showed a significant increase over time from 0.95 to 1.05 SSL (Figure 8j; $R^2 = 0.30$; slope = 3.60×10^{-3}). Even without considering the highest Ŋ value of the time series (2015), the linear regression remained significant. In the transition area, Ŋ also exhibited a significant increase ($R^2 = 0.53$; slope = $2.29.10^{-2}$) (Figure 8j), while the trend in the offshore area was not significant, although an increase from 1995 to 2005 was observed, and reaching an asymptote.

The minimal depth of the shallowest SSL ($đ_1$) decreased over time in the inshore area (Figure 8m) following a third-order pattern, while it remained relatively unchanged in the transition area (Figure 8n) and increased offshore following a third-order pattern (Figure 8o). Interestingly, a discrete hyperbolic pattern emerged in the inshore area, while a parabolic pattern was observed offshore. In both cases, a change in trend direction was again reported during the 2004-2006 period.

The width of the shallowest SSL, $\dot{W}_1$, significantly increased over time in all areas, particularly in the transition and offshore areas. The width increased from 50 m to approximately 80 m (transition, Figure 8q) and 120 m (offshore, Figure 8r), with a first-order polynomial estimate of 235 ($R^2 = 9.71\ 10^{-4}$) and 3,693 ($R^2 = 6.17\ 10^{-2}$) for transition and offshore area, respectively (Table 4). In the inshore area, the trend was not well-defined.

Table 4. Regressions analysis results for sound scattering layers (SSLs) descriptors over years (1995-2015). The polynomial order indicates the best regression ($p < 0.05$) calculated, ranging from 1 and 3. When the polynomial order is 1, the regression is linear. The estimate of first degree (E) represents the estimation of the first-order factor. The R^2 value indicated the adjusted R-squared.

Descriptor \ Area	Inshore	Transition	Offshore
S_v from the whole water column ($S_{v, EI}$)	Order: 3 E: 201.54 $R^2 = 9.84\ 10^{-3}$	Order: 3 E: 154.70 $R^2 = 5.63\ 10^{-2}$	Order: 1 E: 117.42 $R^2 = 6.81\ 10^{-2}$
S_v from the shallowest SSL ($S_{v, 1}$)	Order: 3 E: 55.06 $R^2 = 5.84\ 10^{-3}$	Order: 3 E: 23.53 $R^2 = 1.73\ 10^{-2}$	Order: 3 E: 71.74 $R^2 = 5.82\ 10^{-2}$
S_v from all SSLs ($S_{v, all}$)	Order: 3 E: 49.45 $R^2 = 6.15\ 10^{-3}$	Order: 3 E: -22.21 $R^2 = 8.77\ 10^{-3}$	Order: 3 E: 17.07 $R^2 = 1.65\ 10^{-2}$
Number of SSLs (Ŋ)	Order: 1 E: 9.43 $R^2 = 2.35\ 10^{-3}$	Order: 1 E: 31.24 $R^2 = 1.66\ 10^{-2}$	Order: 3 E: 14.98 $R^2 = 1.20\ 10^{-2}$
Minimal depth of the shallowest SSL (đ$_1$)	Order: 3 E: -144.17 $R^2 = 5.38\ 10^{-3}$	Order: 3 E: non-significant $R^2 = 7.56\ 10^{-3}$	Order: 3 E: -1090.89 $R^2 = 1.43\ 10^{-2}$
Width of the shallowest SSL ($\dot{W}_1$)	Order: 3 E: 235.09 $R^2 = 9.71\ 10^{-4}$	Order: 3 E: 2616.86 $R^2 = 6.05\ 10^{-2}$	Order: 3 E: 3693.94 $R^2 = 6.17\ 10^{-2}$

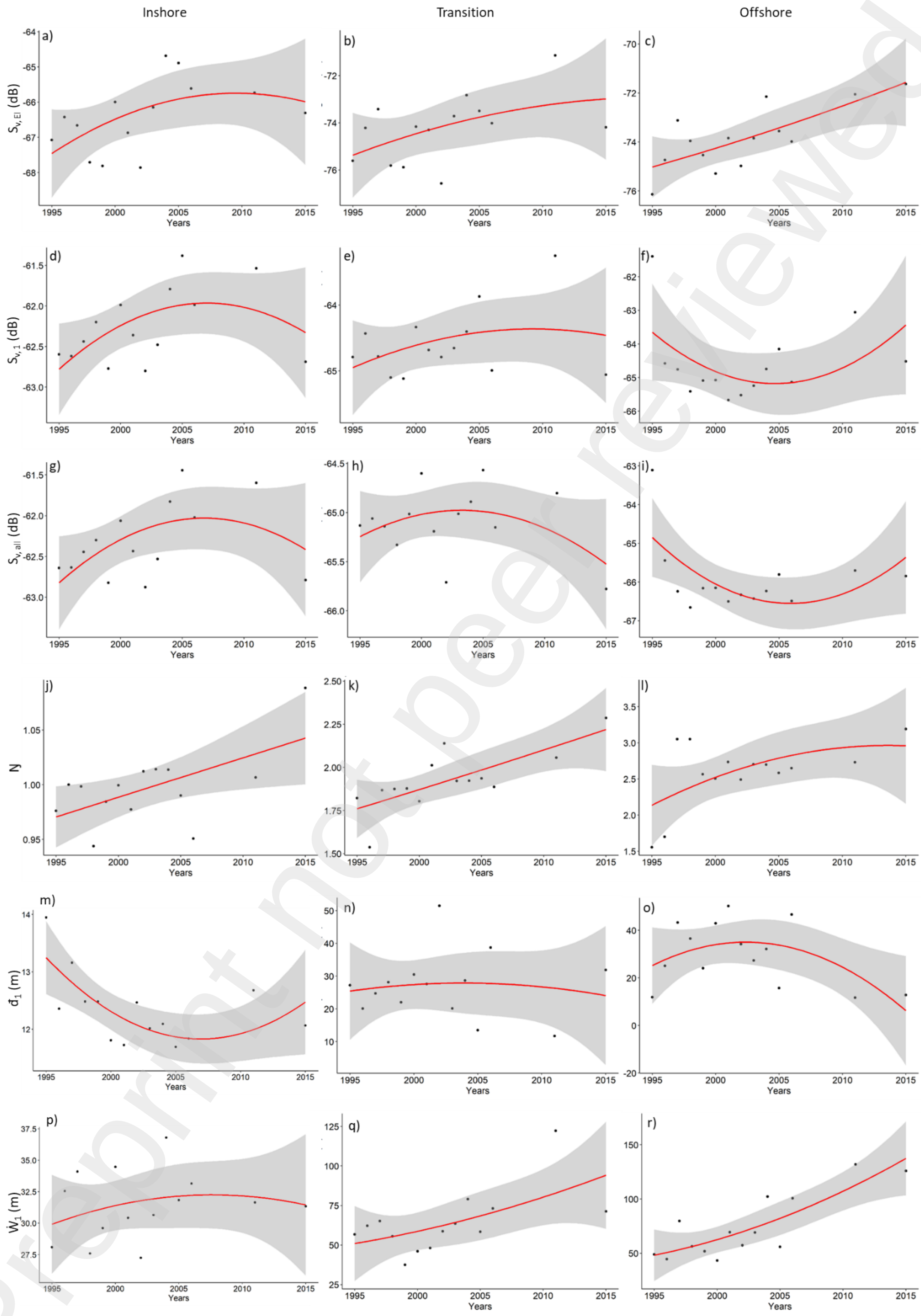

376

377 Figure 8. Temporal patterns of acoustic descriptors surveyed over two decades (1995-2015) in different bathymetric areas.

378 a - c) mean S_v from the whole water column ($S_{v, EI}$ in dB); d - f) mean S_v from the shallowest 'SSL' Sound Scattered Layer ($S_{v,1}$

in dB), and g - i) mean S_v from all SSLs ($S_{v, all}$ in dB); j - l) number of SSL (Ŋ); m - o) minimal depth of the shallowest SSL (đ$_1$ in m); p - r) width of shallowest SSL ($\dot{W}_1$ in m). First column a) d) g) j) m) p) represent the inshore area (bottom depth < 150 m), the second b) e) h) k) n) q) the transition area (bottom depth in 150-500 m) and the third c) f) i) l) o) r) the offshore area (bottom depth > 500 m). Red lines represent significant regression, either linear or polynomial. The grey shade represent the standard error.

4. Discussion

The high number ESUs processed in each bathymetric area enabled reliable comparisons. Few shallow coastal samplings have been carried out, as is typical in fisheries acoustics surveys (Brehmer *et al.*, 2006; David *et al.*, 2024), for safe navigation. The delimitation between the transition and offshore areas can be further refined. We suggest developing an algorithm that takes into account other bathymetric factors, such as the slope, for future studies. The ultra-shallow coastal (< 10m depth) area, including the surf zone, is not investigated in this study and should present some specific characteristics compared to the three bathymetric strata studied.

4.1. Effectiveness of acoustics descriptors to assess pelagic community organisation

The SSL descriptors (Mouget *et al.*, 2022) appeared efficient for monitoring SSLs and nektonic communities, highlighting differences and similarities within the SCCLME between the three studied bathymetric areas. Descriptors from echointegration were complementary to SSL ones. The indicators derived from echointegration ($S_{v, EI}$ by ESU, vertical profiles of $S_{v, EI}$, $S_{v, EI}$ classes) allowed exploration of the different acoustic communities according to their acoustic responses. $S_{v, EI}$ analysis was more exhaustive but required additional computational work, in contrast to SSL descriptors (Mouget *et al.*, 2022), which could be used routinely to compare and monitor the nonspecific spatial organization of pelagic communities in marine ecosystems.

4.2. Comparison of inshore, transition, and offshore pelagic areas using echointegration and SSL descriptors

The observed descriptors reveal significant distinctions in pelagic communities and their vertical distribution across the three bathymetric areas. Notably, pelagic biomass (S_v) is markedly higher in shallower waters, consistent with prior studies highlighting increased abundance of pelagic fish (Brehmer *et al.*, 2006; David *et al.*, 2022) and plankton (Gasol, del Giorgio and Duarte, 1997) in coastal areas. These shallow waters, such as those inhabited by swimbladders fish species like *Clupea harengus*

(Maravelias, 1999) and *Sardinella maderensis* (Sarré *et al.*, 2018), serve as crucial spawning and nursery grounds, exhibiting a high abundance of ichthyoplankton (Tiedemann *et al.*, 2017).

The vertical structuring of pelagic biomass in the water column is linked to the bathymetric area. Although vertical profiles from $S_{v,\ 1}$, $S_{v,\ all}$, and $S_{v,\ EI}$ exhibit peaks at similar values for transition and offshore, their amplitudes differ, while inshore demonstrates a peak for a distinct pelagic biomass. As acoustic responses are species-dependent, inshore communities appear distinct from those in transition and offshore areas. Previous studies have validated the differentiation of communities along bathymetric gradients (Smith and Brown, 2002; Louisy, 2015), suggesting that the varied pelagic biomass (S_v) peaks along bathymetric areas correspond to different species assemblages with similar acoustic responses. The size of the water column, constrained by surface and bottom boundaries, significantly influences inshore areas compared to deeper regions. This constraint can explain the fact that the number of SSLs (Ŋ) exhibits a maximal ratio of ESUs for a single SSL, whereas transition and offshore are similar with a majority of ESUs with two SSLs. However, some other pelagic organizations, such as $đ_1$ and $\dot{W}_1$ (minimal depth and width of the shallowest SSL), remain independent of bathymetric area. This underscores that the shallowest SSL is constrained by environmental parameters, and especially bathymetry (Weston, 1958; Marchal, Gerlotto and Stequert, 1993). The micronektonic organisms of the SSLs establish trophic relationships with primary producers; thus, the size of the SSL (height, surface) could be optimal depending of species organization or simply consistent across bathymetric constraint. The minimal depth of the shallowest SSL is constrained by the thermocline (Diogoul *et al.*, 2020). A portion of SSL remains close to the surface (< 50m) regardless of bathymetry, making them sensitive to ocean surface characteristics (Fig. S1).

Analysis of $S_{v,\ EI}$ vertical profiles confirms differences between inshore *vs.* offshore and transition. The similarity between transition and offshore is primarily observed in the upper part of the water column (0-100 m), indicating that shallower micronektonic community is continuously present whatever the bathymetry. Deeper (>100m), the $S_{v,\ EI}$ of the transition area becomes progressively different from the offshore area with depth. Such difference could be attributed to change(s) in community and/or environment (Diogoul *et al.*, 2020). Inshore $S_{v,\ EI}$ follows the same global pattern as others, albeit slightly shifted, with higher values of S_v. These elevated values could correspond to more pelagic fish, supporting the hypothesis of different species composition but similar organization due to environmental parameters, which vary based on the distance from the coast (Schickele *et al.*, 2020).

Considering the entire water column, each depth category exhibits its own predominant acoustic class ($S_{v,\ EI}$ classes). This result aligns with our findings on pelagic biomass (S_v) of SSLs, where transition and offshore areas are similar. They differ slightly for classes [-60; -50[and [-90; -80[dB, higher for the transition than offshore, possibly due to inshore contiguity with the transition area. The inshore area is characterized by a significant percentage of ESUs over -50 dB: classes [-60; -50[and [-70; -60[dB are highly represented inshore. Higher classes of S_v, [-70; -60[and [-60; -50[correspond to larger organisms such as pelagic fishes, while lower S_v values are indicative of zooplankton (Diogoul *et al.*, 2021). A comparison of inshore and offshore areas highlights differences in fish species composition (Sarré *et al.*, 2018). The acoustic profiles of the transition area are closer to offshore than those of inshore areas, especially the shallowest SSL. Species composition and DVMs are driven, among other environmental parameters, by bottom depth (Macpherson and Duarte, 1991; Collins *et al.*, 2012), revealing structural differences between the three bathymetric areas, which necessitate separate consideration for modelling and monitoring.

4.3. Diel vertical migration according to bathymetric areas

The majority of biomass involved in DVM comprises organisms larger than 1 mm, detected at 38 kHz (Hernández-León *et al.*, 2001; Hernández-León, Gómez and Arístegui, 2007). Our study reveals distinct DVM behavioral differences between inshore and offshore areas, with intermediate signals observed in the transition area. The low correlation between inshore and transition areas likely stems from the divergence of signals around 45 m depth, possibly indicating different species compositions or DVM behaviors in inshore and offshore areas. At least three distinct pelagic communities are apparent: one inshore and two offshore. The positive difference in $đ_1$ between day and night suggests a variable behavioral response of organisms to depth availability and/or variability in species composition within the community.

The inshore community appears more compact during the night, located around 50 m, and more scattered during the daytime. This explains low pelagic biomass (S_v) values and aligns with DVM type I, as mostly reported in the Atlantic Ocean (Hays, 1996). Zooplankton species typically exhibit type I DVM, ascending to the surface during the night and descending to deeper layers during the day (Bianchi *et al.*, 2013; Lehodey *et al.*, 2015; Cascão *et al.*, 2019). The zooplankton community in the CCLME is dominated by copepods (Ariza *et al.*, 2016), and clupeids and their larvae are part of the fish communities in the inshore area (Tiedemann *et al.*, 2017; Sarré *et al.*, 2018). The day-night difference could also be attributed to diel horizontal migrations, with organisms from all three bathymetric areas migrating to more coastal and shallower areas during the night (Benoit-Bird *et al.*, 2001). This phenomenon may explain why pelagic biomass is consistently higher during the night than during the day. However, the difference in biomass could also be due to fish avoiding vessels more in shallow waters than in deeper areas (Brehmer *et al.*, 2006).

Offshore, DVM indicates the presence of two distinct functional groups: one with positive tropism to light and the other with negative tropism. The highest pelagic biomass peak offshore is around 50 m depth during the night, demonstrating the formation of SSL in these areas, during the night unlike the inshore area. A portion of these communities migrates to the surface, and the majority migrates under 250 m depth, likely below the thermocline (Vélez-Bechi *et al.*, 2015). The pelagic biomass difference between night and day is positive from the surface to 250 m, indicating higher acoustic density with more organisms and/or denser communities. This difference is negative under 250 m depth, indicating that communities migrate from the upper part of the water column during the night to the lower part during the day. This type of DVM reflects a negative tropism to light. The most common fish larvae in the tropical Atlantic Ocean are myctophids (Dolar *et al.*, 2003; Gushchin and Corten, 2017; Olivar *et al.*, 2018) and microstomatids (Olivar *et al.*, 2018). In the shallowest part of the water column (0-50 m), a part of the communities migrates to the surface during the daytime. These communities may be constituted by myctophid and microstomatid larvae, which only inhabit the upper zone (0-200 m). In deeper areas, larvae are not found. Therefore, a hypothesis is that myctophid and microstomatid larvae constitute a significant part of observed DVM, migrating from around 50 m during the night to deeper zones during the day. Around 500 m depth, we observe a low difference between day and night, reflecting the absence of DVM behavior in bathypelagic species. Three communities appear in the transition area, combining inshore (scattering during the night) and offshore (migrating to the surface and migrating deeper) characteristics.

DVM plays a crucial role in ecosystems, influencing trophic interactions (Pinti, Andersen and Visser, 2021) and the carbon export flux of the biological pump (Archibald, Siegel and Doney, 2019). Without biological sampling, species composition remains challenging to validate, but studies by Hernández-León, Gómez and Arístegui (2007) and Diogoul *et al.*, (2021) suggest that the zooplankton composition is dominated by copepods in the SCCLME, with a high diversity of fish listed in the area (Ariza *et al.*, 2016; Olivar *et al.*, 2018). Nevertheless, the functioning can be described and is found to differ across the three bathymetric areas considered.

4.4. Inter-annual trends

The significant increase in the number of Sound Scattering Layers (SSLs) (Ŋ) and pelagic biomass ($S_{v,\ EI}$) across all bathymetric areas corresponds to the rise in sea surface temperature (Gómez-Letona *et al.*, 2017; Diogoul *et al.*, 2021) and increased upwelling intensity (Benazzouz, Demarcq and González-Nuevo, 2015) observed during the two decades studied, potentially linked to global climate change. These parameters have the potential to impact the marine food web and may explain the observed inter-annual trends. The increase in Ŋ may result from the fragmentation of existing SSLs. For surface SSLs, this fragmentation could be linked to the strong winds generated by upwelling in the region. However, other parameters should be explored, including physicochemical parameters (Diogoul *et al.*, 2020) and species composition, as changes in species composition can influence SSL depth and dimensions. The significant increase in the width of the shallowest SSL ($\dot{W}_1$) observed in both transition and offshore areas suggests an increase in the size of these SSLs, indicating a probable increase in their pelagic biomass (Fig. S2).

The offshore area exhibited a distinct significant trend over the years, with $S_{v,\ EI}$ significantly increasing, a phenomenon not observed in other areas. Moreover, $S_{v,\ 1}$ from the shallowest SSL appeared to remain stable over the years. These results align with those of (Diogoul *et al.*, 2021), suggesting that marine pelagic resources, mainly fish and plankton in the continental shelf of the SCCLME, have remained relatively stable over the last two decades. Therefore, the observed increase in pelagic biomass was not solely due to aggregated organisms in SSLs but encompassed the entire water column. Two possible explanations for this phenomenon warrant further exploration: changes in species composition or alterations in schooling behaviour (Brehmer *et al.*, 2007).

Three parameters ($S_{v,\ 1}$, $S_{v,\ all}$, and $đ_1$) exhibited fluctuations along the time series, with alternating periods of increase and decrease, suggesting a cyclic phenomenon with a periodicity of approximately 10 years. These well-known cyclic patterns (*e.g.* Kawasaki, 1992; Bertrand *et al.*, 2004) impact pelagic communities at the decadal scale. The fluctuations are attributed to organism life cycles (Kawasaki, 1992) and environmental factors such as ocean oscillations (Knight, Folland and Scaife, 2006; Alexander, Halimeda Kilbourne and Nye, 2014). The multi-decadal oscillations of the Atlantic Ocean (Schlesinger and Ramankutty, 1994) have known impacts on ecosystem functioning (Edwards *et al.*, 2013; Nye *et al.*, 2014) and SSL structures (Hays, Richardson and Robinson, 2005). The long-term dataset in this study has highlighted the responses of SSLs, as indicated by pelagic biomass ($S_{v,1}$ and $S_{v,\ all}$) and minimal depth ($đ_1$), to these cyclical ocean oscillations. For instance, the $S_{v,1}$ in the inshore area displayed an increase from 1995 to 2005 followed by a decrease from 2005 to 2015, which is the same variation that heat content anomalies observed in the Atlantic over the past decades (NOAA PSL, 2023). Moreover, these oscillations are known to impact pelagic ecosystems, including fish and zooplankton (Alheit *et al.*, 2014), which is observable in the SSLs.

5. Conclusion

By studying the effect of bathymetry on pelagic spatial organization, we found that SSL descriptors were effective in monitoring SSLs and pelagic micronektonic communities, and echointegration descriptors provided useful complementary information. The study recommends using SSL descriptors to monitor the non-specific spatial organization of pelagic communities in marine ecosystems. These findings have implications for future studies on the distribution and behavior of marine organisms in LMEs. This information is useful for refining our understanding of the fine-scale spatial distribution of marine organisms and their habitat preferences.

Higher acoustic pelagic biomass was noted in shallower waters, revealing a distinct correlation between the vertical structure of the water column and the bathymetric area. These findings highlight the importance of considering separate bathymetric areas within LMEs as distinct communities, exhibiting diverse spatial structures and DVM behaviors. Moreover, our results indicate the potential implications of these findings on various biological processes, such as the biological carbon pump and trophic interactions within such ecosystems. By acknowledging the variability between inshore and offshore areas, LME studies can better account for the unique characteristics and dynamics of each bathymetric area. This knowledge is essential for understanding and predicting ecosystem-level processes and for informing effective conservation and management strategies. Furthermore, it underscores the need for targeted research and monitoring efforts that capture the complexity and heterogeneity of LMEs. Overall, our study sheds light on the intricate relationships between bathymetric areas, community dynamics, and key ecological processes. These findings emphasize the significance of incorporating spatial considerations into future LME studies and provide a foundation for further investigations into the functioning and resilience of these valuable marine ecosystems.

6. Acknowledgments

This work was done within the AWA “Ecosystem Approach to the management of fisheries and the marine environment in West African waters” project funded by IRD and the BMBF (grant 01DG12073E and 01DG12073B), www.awa.ird.fr (SRFC: Sub Regional Fisheries Commission) and the PREFACE project funded by the European Commission’s Seventh Framework Program (2007-2013) under Grant Agreement number 603521, https://preface.b.uib.no/ and ended within TriAtlas European project grant number 817578 and nextGEMS funded through the European Union’s Horizon 2020 research and innovation program under the grant agreement number 101003470. We thank the Nansen project (FAO/IMR), Dr Jens-Otto Krakstad (IMR, Norway) as FAO, and African colleagues for data collection, particularly Salahedine El-Ayoubi (INRH, Morocco). This work has also been supported by ARED funding from the Brittany region (France). We thank Pr. Eric Feunteun (MNHN, France) for the advices and review.

References

Alexander, M.A., Halimeda Kilbourne, K. and Nye, J.A. (2014) ‘Climate variability during warm and cold phases of the Atlantic Multidecadal Oscillation (AMO) 1871–2008’, *Journal of Marine Systems*, 133, pp. 14–26. Available at: https://doi.org/10.1016/j.jmarsys.2013.07.017.

Alheit, J. *et al.* (2014) ‘Reprint of “Atlantic Multidecadal Oscillation (AMO) modulates dynamics of small pelagic fishes and ecosystem regime shifts in the eastern North and Central Atlantic”’, *Journal of Marine Systems*, 133, pp. 88–102. Available at: https://doi.org/10.1016/j.jmarsys.2014.02.005.

Archibald, K.M., Siegel, D.A. and Doney, S.C. (2019) ‘Modeling the Impact of Zooplankton Diel Vertical Migration on the Carbon Export Flux of the Biological Pump’, *Global Biogeochemical Cycles*, 33(2), pp. 181–199. Available at: https://doi.org/10.1029/2018GB005983.

Arístegui, J. *et al.* (2009) ‘Sub-regional ecosystem variability in the Canary Current upwelling’, *Progress in Oceanography*, 83(1), pp. 33–48. Available at: https://doi.org/10.1016/j.pocean.2009.07.031.

Ariza, A. *et al.* (2016) ‘Vertical distribution, composition and migratory patterns of acoustic scattering layers in the Canary Islands’, *Journal of Marine Systems*, 157, pp. 82–91. Available at: https://doi.org/10.1016/j.jmarsys.2016.01.004.

Ariza, A. *et al.* (2022) ‘Global decline of pelagic fauna in a warmer ocean’, *Nature Climate Change*, 12(10), pp. 928–934. Available at: https://doi.org/10.1038/s41558-022-01479-2.

Auger, P.-A. *et al.* (2016) ‘What drives the spatial variability of primary productivity and matter fluxes in the north-west African upwelling system? A modelling approach’, *Biogeosciences*, 13(23), pp. 6419–6440. Available at: https://doi.org/10.5194/bg-13-6419-2016.

Barton, E.D. *et al.* (1998) ‘The transition zone of the Canary Current upwelling region’, *Progress in Oceanography*, 41(4), pp. 455–504. Available at: https://doi.org/10.1016/S0079-6611(98)00023-8.

Barton, E.D., Field, D.B. and Roy, C. (2013) ‘Canary current upwelling: More or less?’, *Progress in Oceanography*, 116, pp. 167–178. Available at: https://doi.org/10.1016/j.pocean.2013.07.007.

Beaugrand, G., Ibañez, F. and Reid, P.C. (2000) ‘Spatial, seasonal and long-term fluctuations of plankton in relation to hydroclimatic features in the English Channel, Celtic Sea and Bay of Biscay’, *Marine Ecology Progress Series*, 200, pp. 93–102. Available at: https://doi.org/10.3354/meps200093.

Béhagle, N. *et al.* (2014) ‘Mesoscale features and micronekton in the Mozambique Channel: An acoustic approach’, *Deep Sea Research Part II: Topical Studies in Oceanography*, 100, pp. 164–173. Available at: https://doi.org/10.1016/j.dsr2.2013.10.024.

Béhagle, N. *et al.* (2016) ‘Acoustic micronektonic distribution is structured by macroscale oceanographic processes across 20–50°S latitudes in the South-Western Indian Ocean’, *Deep Sea Research Part I: Oceanographic Research Papers*, 110, pp. 20–32. Available at: https://doi.org/10.1016/j.dsr.2015.12.007.

Béhagle, N. *et al.* (2017) ‘Acoustic distribution of discriminated micronektonic organisms from a bi-frequency processing: The case study of eastern Kerguelen oceanic waters’, *Progress in Oceanography*, 156, pp. 276–289. Available at: https://doi.org/10.1016/j.pocean.2017.06.004.

Benazzouz, A. *et al.* (2014) 'An improved coastal upwelling index from sea surface temperature using satellite-based approach – The case of the Canary Current upwelling system', *Continental Shelf Research*, 81, pp. 38–54. Available at: https://doi.org/10.1016/j.csr.2014.03.012.

Benazzouz, A., Demarcq, H. and González-Nuevo, G. (2015) 'Recent changes and trends of the upwelling intensity in the Canary Current Large Marine Ecosystem', in L. Valdés and I. Déniz-Gonzalez (eds) *Oceanographic and biological features in the Canary Current Large Marine Ecosystem*. Paris: IOC-UNESCO, pp. 321–330. Available at: http://hdl.handle.net/1834/9198 (Accessed: 19 May 2022).

Benoit-Bird, K. *et al.* (2001) 'Diel horizontal migration of the Hawaiian mesopelagic boundary community observed acoustically', *Marine Ecology Progress Series*, 217, pp. 1–14. Available at: https://doi.org/10.3354/meps217001.

Benoit-Bird, K.J. and Au, W.W.L. (2004) 'Diel migration dynamics of an island-associated sound-scattering layer', *Deep Sea Research Part I: Oceanographic Research Papers*, 51(5), pp. 707–719. Available at: https://doi.org/10.1016/j.dsr.2004.01.004.

Bertrand, A. *et al.* (2004) 'From small-scale habitat loopholes to decadal cycles: a habitat-based hypothesis explaining fluctuation in pelagic fish populations off Peru', *Fish and Fisheries*, 5(4), pp. 296–316. Available at: https://doi.org/10.1111/j.1467-2679.2004.00165.x.

Bianchi, D. *et al.* (2013) 'Diel vertical migration: Ecological controls and impacts on the biological pump in a one-dimensional ocean model: DIEL VERTICAL MIGRATION IMPACTS', *Global Biogeochemical Cycles*, 27(2), pp. 478–491. Available at: https://doi.org/10.1002/gbc.20031.

Blanluet, A. *et al.* (2019) 'Characterization of sound scattering layers in the Bay of Biscay using broadband acoustics, nets and video', *PLoS ONE*, 14(10). Available at: https://doi.org/10.1371/journal.pone.0223618.

Brehmer, P. *et al.* (2006) 'Evidence of a variable "unsampled" pelagic fish biomass in shallow water (<20 m): the case of the Gulf of Lion', *ICES Journal of Marine Science*, 63(3), pp. 444–451. Available at: https://doi.org/10.1016/j.icesjms.2005.10.016.

Brehmer, P. *et al.* (2007) 'Schooling behaviour of small pelagic fish: phenotypic expression of independent stimuli', *Marine Ecology Progress Series*, 334, pp. 263–272. Available at: https://doi.org/10.3354/meps334263.

Brehmer, P. *et al.* (2019) 'Towards an Autonomous Pelagic Observatory: Experiences from Monitoring Fish Communities around Drifting FADs', *Thalassas: An International Journal of Marine Sciences*, 35(1), pp. 177–189. Available at: https://doi.org/10.1007/s41208-018-0107-9.

Brunel, T. and Boucher, J. (2007) 'Long-term trends in fish recruitment in the north-east Atlantic related to climate change', *Fisheries Oceanography*, 16(4), pp. 336–349. Available at: https://doi.org/10.1111/j.1365-2419.2007.00435.x.

Cascão, I. *et al.* (2019) 'Seamount effects on the diel vertical migration and spatial structure of micronekton', *Progress in Oceanography*, 175, pp. 1–13. Available at: https://doi.org/10.1016/j.pocean.2019.03.008.

Castillo, S., Ramil, F. and Ramos, A. (2017) 'Composition and Distribution of Epibenthic and Demersal Assemblages in Mauritanian Deep-Waters', in A. Ramos, F. Ramil, and J.L. Sanz (eds) *Deep-Sea Ecosystems Off Mauritania: Research of Marine Biodiversity and Habitats in the Northwest African*

Margin. Dordrecht: Springer Netherlands, pp. 317–353. Available at: https://doi.org/10.1007/978-94-024-1023-5_8.

Collins, M.A. *et al.* (2012) ‘Latitudinal and bathymetric patterns in the distribution and abundance of mesopelagic fish in the Scotia Sea’, *Deep Sea Research Part II: Topical Studies in Oceanography*, 59–60, pp. 189–198. Available at: https://doi.org/10.1016/j.dsr2.2011.07.003.

Croux, C. and Dehon, C. (2010) ‘Influence functions of the Spearman and Kendall correlation measures’, *Statistical Methods & Applications*, 19(4), pp. 497–515. Available at: https://doi.org/10.1007/s10260-010-0142-z.

David, V. *et al.* (2022) ‘Insights from a multibeam echosounder to survey pelagic fish shoals and their spatio-temporal distribution in ultra-shallow waters’, *Estuarine, Coastal and Shelf Science*, 264, p. 107705. Available at: https://doi.org/10.1016/j.ecss.2021.107705.

David, V. *et al.* (2024) ‘Species identification of fish shoals using coupled split-beam and multibeam echosounders and two scuba-diving observational methods’, *Journal of Marine Systems*, 241, p. 103905. Available at: https://doi.org/10.1016/j.jmarsys.2023.103905.

Diankha, O. *et al.* (2017) ‘Studying the contribution of different fishing gears to the *Sardinella* small-scale fishery in Senegalese waters’, *Aquatic Living Resources*, 30, p. 27. Available at: https://doi.org/10.1051/alr/2017027.

Diogoul, N. *et al.* (2020) ‘Fine-scale vertical structure of sound-scattering layers over an east border upwelling system and its relationship to pelagic habitat characteristics’, *Ocean Science*, 16(1), pp. 65–81. Available at: https://doi.org/10.5194/os-16-65-2020.

Diogoul, N. *et al.* (2021) ‘On the robustness of an eastern boundary upwelling ecosystem exposed to multiple stressors’, *Scientific Reports*, 11(1), p. 12. Available at: https://doi.org/10.1038/s41598-021-81549-1.

Dolar, M.L.L. *et al.* (2003) ‘COMPARATIVE FEEDING ECOLOGY OF SPINNER DOLPHINS (STENELLA LONGIROSTRIS) AND FRASER’S DOLPHINS (LAGENODELPHIS HOSEI) IN THE SULU SEA’, *Marine Mammal Science*, 19(1), pp. 1–19. Available at: https://doi.org/10.1111/j.1748-7692.2003.tb01089.x.

Domokos, R. (2009) ‘Environmental effects on forage and longline fishery performance for albacore (Thunnus alalunga) in the American Samoa Exclusive Economic Zone’, *Fisheries Oceanography*, 18(6), pp. 419–438. Available at: https://doi.org/10.1111/j.1365-2419.2009.00521.x.

Edwards, M. *et al.* (2013) ‘Marine Ecosystem Response to the Atlantic Multidecadal Oscillation’, *PLoS ONE*. Edited by I. Álvarez, 8(2), p. e57212. Available at: https://doi.org/10.1371/journal.pone.0057212.

Fay, M.P. and Proschan, M.A. (2010) ‘Wilcoxon-Mann-Whitney or t-test? On assumptions for hypothesis tests and multiple interpretations of decision rules’, *Statistics Surveys*, 4(0), pp. 1–39. Available at: https://doi.org/10.1214/09-SS051.

Faye, S. *et al.* (2015) ‘A model study of the seasonality of sea surface temperature and circulation in the Atlantic North-eastern Tropical Upwelling System’, *Frontiers in Physics*, 3. Available at: https://www.frontiersin.org/article/10.3389/fphy.2015.00076 (Accessed: 19 May 2022).

Foote, K.G. *et al.* (1987) *Calibration of acoustic instruments for fish density estimation : a practical guide*. Technical Report 144. ICES Cooperative, pp. 1–69.

Gasol, J.M., del Giorgio, P.A. and Duarte, C.M. (1997) 'Biomass distribution in marine planktonic communities', *American Society of Limnology and Oceanography*, 42(6), pp. 1353–1363.

Gibson, R.N., Atkinson, R.J.A. and Gordon, J.D.M. (eds) (2005) 'Zonation of Deep Biota on Continental Margins', in *Oceanography and Marine Biology*. 0 edn. CRC Press, pp. 221–288. Available at: https://doi.org/10.1201/9781420037449-8.

Gómez-Letona, M. *et al.* (2017) 'Trends in Primary Production in the Canary Current Upwelling System—A Regional Perspective Comparing Remote Sensing Models', *Frontiers in Marine Science*, 4. Available at: https://www.frontiersin.org/article/10.3389/fmars.2017.00370 (Accessed: 19 May 2022).

Görlitz, S. and Interwies, E. (2013) 'Protection of the Canary Current Large Marine Ecosystem (CCLME) - Economic and Social Valuation of the CCLME Ecosystem Services'.

Gushchin, A.V. and Corten, A. (2017) 'Feeding of pelagic fish in waters of Mauritania: 3.—Atlantic Chub mackerel Scomber colias, Atlantic horse mackerel Trachurus trachurus, Cunene horse mackerel Trachurus trecae', *Journal of Ichthyology*, 57(3), pp. 410–423. Available at: https://doi.org/10.1134/S0032945217030067.

Hays, G.C. (1996) 'Large-scale patterns of diel vertical migration in the North Atlantic', *Deep Sea Research Part I: Oceanographic Research Papers*, 43(10), pp. 1601–1615. Available at: https://doi.org/10.1016/S0967-0637(96)00078-7.

Hays, G.C., Richardson, A.J. and Robinson, C. (2005) 'Climate change and marine plankton', *Trends in Ecology & Evolution*, 20(6), pp. 337–344. Available at: https://doi.org/10.1016/j.tree.2005.03.004.

Hedger, R. *et al.* (2004) 'Analysis of the spatial distributions of mature cod (Gadus morhua) and haddock (Melanogrammus aeglefinus) abundance in the North Sea (1980–1999) using generalised additive models', *Fisheries Research*, 70(1), pp. 17–25. Available at: https://doi.org/10.1016/j.fishres.2004.07.002.

Hernández-León, S. *et al.* (2001) 'Vertical distribution of zooplankton in Canary Island waters: implications for export flux', *Deep Sea Research Part I: Oceanographic Research Papers*, 48(4), pp. 1071–1092. Available at: https://doi.org/10.1016/S0967-0637(00)00074-1.

Hernández-León, S., Gómez, M. and Arístegui, J. (2007) 'Mesozooplankton in the Canary Current System: The coastal–ocean transition zone', *Progress in Oceanography*, 74(2), pp. 397–421. Available at: https://doi.org/10.1016/j.pocean.2007.04.010.

Holland, M.M. *et al.* (2021) 'Characterizing the three-dimensional distribution of schooling reef fish with a portable multibeam echosounder', *Limnology and Oceanography: Methods*, 19(5), pp. 340–355. Available at: https://doi.org/10.1002/lom3.10427.

Huan, Y. *et al.* (2022) 'Phytoplankton Size Classes in the Global Ocean at Different Bathymetric Depths', *IEEE Transactions on Geoscience and Remote Sensing*, 60, pp. 1–11. Available at: https://doi.org/10.1109/TGRS.2022.3153477.

Kaschner, K. *et al.* (2006) 'Mapping world-wide distributions of marine mammal species using a relative environmental suitability (RES) model', *Marine Ecology Progress Series*, 316, pp. 285–310. Available at: https://doi.org/10.3354/meps316285.

Kawasaki, T. (1992) ‘Mechanisms governing fluctuations in pelagic fish populations’, *South African Journal of Marine Science*, 12(1), pp. 873–879. Available at: https://doi.org/10.2989/02577619209504748.

Knight, J.R., Folland, C.K. and Scaife, A.A. (2006) ‘Climate impacts of the Atlantic Multidecadal Oscillation’, *Geophysical Research Letters*, 33(17). Available at: https://doi.org/10.1029/2006GL026242.

Lehodey, P. *et al.* (2015) ‘Optimization of a micronekton model with acoustic data’, *ICES Journal of Marine Science*, 72(5), pp. 1399–1412. Available at: https://doi.org/10.1093/icesjms/fsu233.

Lenoir, S., Beaugrand, G. and Lecuyer, É. (2011) ‘Modelled spatial distribution of marine fish and projected modifications in the North Atlantic Ocean’, *Global Change Biology*, 17(1), pp. 115–129. Available at: https://doi.org/10.1111/j.1365-2486.2010.02229.x.

Louisy, P. (2015) *Guide d’identification des poissons marins: Europe et Méditerranée*. 3e éd. entièrement revue, complétée et mise à jour. Paris: Ulmer.

MacLennan, D.N., Fernandes, P.G. and Dalen, J. (2002) ‘A consistent approach to definitions and symbols in fisheries acoustics’, *ICES Journal of Marine Science*, 59(2), pp. 365–369. Available at: https://doi.org/10.1006/jmsc.2001.1158.

Macpherson, E. and Duarte, C.M. (1991) ‘Bathymetric trends in demersal fish size: is there a general relationship?’, *Marine Ecology Progress Series*, 71(2), pp. 103–112.

Majewski, A.R. *et al.* (2017) ‘Marine fish community structure and habitat associations on the Canadian Beaufort shelf and slope’, *Deep Sea Research Part I: Oceanographic Research Papers*, 121, pp. 169–182. Available at: https://doi.org/10.1016/j.dsr.2017.01.009.

Maravelias, C.D. (1999) ‘Habitat selection and clustering of a pelagic fish: effects of topography and bathymetry on species dynamics’, *Canadian Journal of Fisheries and Aquatic Sciences*, 56(3), pp. 437–450. Available at: https://doi.org/10.1139/f98-176.

Marchal, E., Gerlotto, F. and Stequert, B. (1993) ‘On the relationship between scattering layer, thermal structure and tuna abundance in the eastern atlantic equatorial current system’, *Oceanologica Acta*, 16(3), pp. 261–272.

McHugh, M.L. (2013) ‘The Chi-square test of independence’, *Biochemia medica : Biochemia medica*, 23(2), pp. 143–149. Available at: https://doi.org/10.11613/BM.2013.018.

Mouget, A. *et al.* (2022) ‘Applying Acoustic Scattering Layer Descriptors to Depict Mid-Trophic Pelagic Organisation: The Case of Atlantic African Large Marine Ecosystems Continental Shelf’, *Fishes*, 7(2), p. 86. Available at: https://doi.org/10.3390/fishes7020086.

NOAA PSL (2023) ‘Kaplan Extanded SST V2, data provided by the NOAA PSL, Boulder, Colorado’. Available at: https://psl.noaa.gov/ (Accessed: 21 July 2023).

Nye, J.A. *et al.* (2014) ‘Ecosystem effects of the Atlantic Multidecadal Oscillation’, *Journal of Marine Systems*, 133, pp. 103–116. Available at: https://doi.org/10.1016/j.jmarsys.2013.02.006.

Olivar, M.P. *et al.* (2018) ‘Variation in the diel vertical distributions of larvae and transforming stages of oceanic fishes across the tropical and equatorial Atlantic’, *Progress in Oceanography*, 160, pp. 83–100. Available at: https://doi.org/10.1016/j.pocean.2017.12.005.

Perrot, Y. *et al.* (2018) ‘Matecho: An Open-Source Tool for Processing Fisheries Acoustics Data’, *Acoustics Australia* [Preprint]. Available at: https://doi.org/10.1007/s40857-018-0135-x.

Pinti, J., Andersen, K.H. and Visser, A.W. (2021) ‘Co-adaptive behavior of interacting populations in a habitat selection game significantly impacts ecosystem functions’, *Journal of Theoretical Biology*, 523, p. 110663. Available at: https://doi.org/10.1016/j.jtbi.2021.110663.

R Core Team (2021) ‘R: A language and environment for statistical computing’. Vienna, Austria: R Foundation for Statistical Computing. Available at: https://www.R-project.org/.

Remond, B. (2015) *Les couches diffusantes du golfe de Gascogne : caractérisation acoustique, composition spécifique et distribution spatiale*. Available at: http://www.theses.fr/2015PA066076/document.

Sabarros, P.S. *et al.* (2009) ‘Mesoscale eddies influence distribution and aggregation patterns of micronekton in the Mozambique Channel’, *Marine Ecology Progress Series*, 395, pp. 101–107.

Sarré, A. *et al.* (2018) ‘Spatial distribution of main clupeid species in relation to acoustic assessment surveys in the continental shelves of Senegal and The Gambia’, *Aquatic Living Resources*, 31, p. 9. Available at: https://doi.org/10.1051/alr/2017049.

Schickele, A. *et al.* (2020) ‘Modelling European small pelagic fish distribution: Methodological insights’, *Ecological Modelling*, 416, p. 108902. Available at: https://doi.org/10.1016/j.ecolmodel.2019.108902.

Schlesinger, M.E. and Ramankutty, N. (1994) ‘An oscillation in the global climate system of period 65–70 years’, *Nature*, 367(6465), pp. 723–726.

Sheather, S.J. and Jones, M.C. (1991) ‘A Reliable Data-Based Bandwidth Selection Method for Kernel Density Estimation’, *Journal of the Royal Statistical Society. Series B (Methodological)*, 53(3), pp. 683–690.

Sherman, K. (1994) ‘Sustainability, biomass yields, and health of coastal ecosystems: an ecological perspective’, 112, pp. 277–301.

Simmonds, E.J. and MacLennan, D.N. (2005) *Fisheries acoustics: theory and practice*. 2nd ed. Oxford ; Ames, Iowa: Blackwell Science (Fish and aquatic resources series, 10).

Smith, K.F. and Brown, J.H. (2002) ‘Patterns of diversity, depth range and body size among pelagic fishes along a gradient of depth’, *Global Ecology and Biogeography*, 11(4), pp. 313–322. Available at: https://doi.org/10.1046/j.1466-822X.2002.00286.x.

Spall, M.A. (1990) ‘Circulation in the Canary Basin: A model/data analysis’, *Journal of Geophysical Research: Oceans*, 95(C6), pp. 9611–9628. Available at: https://doi.org/10.1029/JC095iC06p09611.

Tiedemann, M. *et al.* (2017) ‘Does upwelling intensity determine larval fish habitats in upwelling ecosystems? The case of Senegal and Mauritania’, *Fisheries Oceanography*, 26(6), pp. 655–667. Available at: https://doi.org/10.1111/fog.12224.

Urmy, S.S., Horne, J.K. and Barbee, D.H. (2012) ‘Measuring the vertical distributional variability of pelagic fauna in Monterey Bay’, *ICES Journal of Marine Science*, 69(2), pp. 184–196. Available at: https://doi.org/10.1093/icesjms/fsr205.

Vélez-Bechi, P. *et al.* (2015) ‘Open ocean temperature and salinity trends in the Canary Current Large Marine Ecosystem’, *IOC Technical Series*, Oceanographic and biological features in the Canary Current Large Marine Ecosystem(115), pp. 299–309.

Weill, A., Scalabrin, C. and Diner, N. (1993) ‘MOVIES-B: an acoustic detection description software. Application to shoal species’ classification’, *Aquatic Living Resources*, 6(3), pp. 255–267. Available at: https://doi.org/10.1051/alr:1993026.

Weston, D.E. (1958) ‘Observations on a scattering layer at the thermocline’, *Deep Sea Research (1953)*, 5(1), pp. 44–50. Available at: https://doi.org/10.1016/S0146-6291(58)80007-7.

Woillez, M. *et al.* (2007) ‘Indices for capturing spatial patterns and their evolution in time, with application to European hake (Merluccius merluccius) in the Bay of Biscay’, *ICES Journal of Marine Science*, 64(3), pp. 537–550. Available at: https://doi.org/10.1093/icesjms/fsm025.

Zhang, G. *et al.* (2018) ‘Modelling species habitat suitability from presence-only data using kernel density estimation’, *Ecological Indicators*, 93, pp. 387–396. Available at: https://doi.org/10.1016/j.ecolind.2018.04.002.

Supplementary material

Appendix 1: đ$_1$ depending of the bottom depth

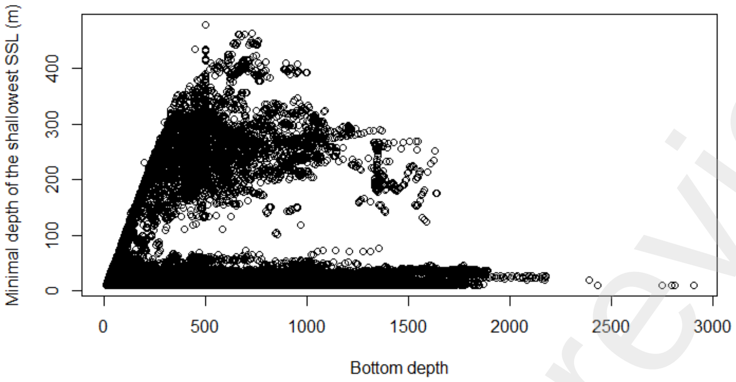

Figure S1. Repartition of đ$_1$ the minimal depth of the shallowest sound scattering layer (SSL) depending of the bottom depth.

Appendix 2: Inter-annual trends of $S_{a,\ all}$

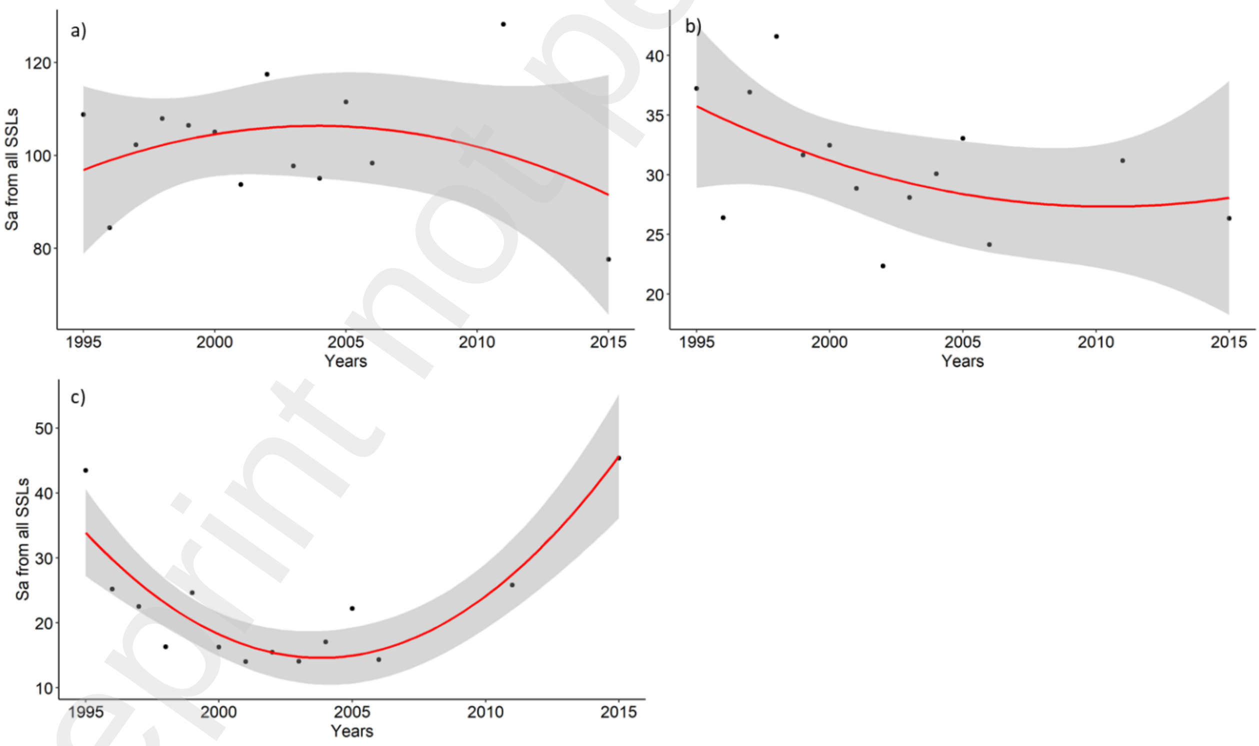

Figure S2. Mean per year over the two decades studied period (1995-2015) mean area backscattering strength S_a from the whole water on a) inshore (bottom depth < 150 m), b) transition (bottom depth in 150-500 m) and c) offshore (bottom depth > 500 m). Red lines represent significant polynomial regressions.